

First-principles description of phonons in Ni₅₀Pt₅₀ disordered alloys: The role of relaxation

Subhradip Ghosh,* J. B. Neaton,[†] Armin H. Antons,[‡] Morrel H. Cohen, and P. L. Leath
*Department of Physics and Astronomy, Rutgers, the State University of New Jersey, 136 Frelinghuysen Road, Piscataway,
 New Jersey 08854-8019, USA*

(Received 10 March 2004; published 22 July 2004)

Using a combination of density-functional perturbation theory and the itinerant coherent potential approximation, we study the effects of atomic relaxation on the inelastic incoherent neutron scattering cross sections of disordered Ni₅₀Pt₅₀ alloys. We build on previous work, where empirical force constants were adjusted *ad hoc* to agree with experiment. After first relaxing all structural parameters within the local-density approximation for ordered NiPt compounds, density-functional perturbation theory is then used to compute phonon spectra, densities of states, and force constants. The resulting nearest-neighbor force constants are first compared to those of other ordered structures of different stoichiometry and then used to generate the inelastic scattering cross sections within the itinerant coherent potential approximation. We find that structural relaxation substantially affects the computed force constants and resulting inelastic cross sections, and that the effect is much more pronounced in random alloys than in ordered alloys.

DOI: 10.1103/PhysRevB.70.024206

PACS number(s): 72.10.Di

I. INTRODUCTION

Extensive experimental studies of the lattice dynamics of random binary alloys over the past 40 years¹⁻⁵ have provided considerable insight into the nature of their elementary excitations. Compared with ordered alloys, the presence of disorder results in different phenomena that depend on the impurity concentration but also crucially on both the relative mass and size differences between the constituents. For large mass or size differences, the effect of disorder can be dramatic, such as the appearance of sharp discontinuities (or split bands) observed in the dispersion.

Among disordered alloys, the Ni_xPt_{1-x} system has been especially well studied experimentally.⁶⁻⁸ Structurally simple, the system assumes variants of the fcc structure over a wide composition range; moreover, the components have large mass ($M_{\text{Pt}}/M_{\text{Ni}}=3.323$) and size ($r_{\text{Pt}}/r_{\text{Ni}}=1.12$) ratios. Further, the phonons of the end point compounds, elemental metallic Pt and Ni, have also been well characterized both experimentally and theoretically.⁶⁻⁸ The interest in these alloys has arisen in part because homogeneous crystals are easy to grow at nearly any concentration, making the system attractive for experimental study.

Theoretically, there have been many attempts to describe the complex nature of phonon excitations in random alloys. The majority were based on the coherent potential approximation⁹ (CPA) and its various generalizations.¹⁰⁻¹⁷ The CPA is a single-site, mean-field theory capable of dealing only with mass disorder; it is commonly generalized to treat both off-diagonal and environmental disorder. A translationally invariant CPA based on the augmented space formalism¹⁸ has recently been used successfully to describe the lattice dynamics of Ni₅₅Pd₄₅ and Ni₅₀Pt₅₀ random alloys.¹⁹ This formalism, known as the itinerant CPA (or ICPA), captures the effects of both force constant *and* mass disorder.

A key deficiency of the application of those theories is that the Green's functions are constructed from *empirical*

force constants. Moreover, in Ref. 19 the empirical force constants were then themselves adjusted to fit frequencies and linewidths extracted from neutron-scattering data. A better alternative to reliance on phenomenological force constants is to compute them from first principles. In recent years, first-principles density-functional theory (DFT) has achieved the ability to predict material properties accurately without experimental input or adjustable parameters. A wealth of first-principles studies has demonstrated that electronic, vibrational, and transport properties are often extremely sensitive to the precise details of the atomic arrangement.²⁰⁻²⁴ Providing a parameter-free description of the vibrational properties of binary alloys would allow a deeper, atomic-scale understanding of the phenomenology.

An especially relevant atomic-scale aspect of these disordered alloys which can be captured by first-principles methods is the degree to which the atoms displace from their high-symmetry fcc sites because of size mismatch; these atomic "relaxations" would be expected to have considerable impact on the force constants. Experimentally, non-negligible displacements are routinely found in binary alloys where the size difference between the constituents is large. For example, extended x-ray-absorption fine structure (EXAFS) measurements of CuPd alloys have shown that 1 at. % Pd in Cu changes the Cu-Pd nearest-neighbor distance to 2.560 Å, from the 2.515 Å Cu-Cu bond distance in pure Cu.²⁵ Another EXAFS study of the Ni_xAu_{1-x} system revealed three distinct Ni-Ni, Au-Au, and Ni-Au bond lengths.²⁶

Within the first-principles framework, some degree of translational symmetry is almost always assumed and disordered systems, such as random binary alloys, are treated approximately, usually by averaging properties over several different ordered atomic configurations. Current computational capabilities limit the size of each configuration, or *supercell*, and also the number of configurations sampled. However, information from one particular ordered compound can nonetheless provide insight into the physics of its disordered counterparts. Although the force constants of a particular ordered system are not necessarily expected to be trans-

ferable to a random environment, they should yield insight into the relative contribution of lattice composition and relaxation to the vibrational properties of $\text{Ni}_{50}\text{Pt}_{50}$, a fundamental feature of these systems which has yet to be studied.

In this article, we attempt to capture the effects of atomic relaxation on the inelastic incoherent neutron-scattering cross section of disordered $\text{Ni}_{50}\text{Pt}_{50}$ using first-principles force constants computed from ordered alloys as input to the ICPA. We build on previous work with the ICPA in which empirical force constants were adjusted in an *ad hoc* manner to agree with experimental cross section spectra.¹⁹ With a large mass and size ratio, $\text{Ni}_{50}\text{Pt}_{50}$ is expected to possess substantial atomic relaxation and large force constant ratios; further, we have a wealth of experimental and theoretical results for comparison.

The paper is organized as follows. In Sec. II, we briefly describe the theoretical tools used in this work to connect the first-principles calculations with the random alloy systems. In Sec. III, we present phonon spectra, site-projected phonon densities of states, and force constant results for the ordered $\text{Ni}_{50}\text{Pt}_{50}$ compounds in pseudocubic and $L10$ structures; the force constants of $\text{Ni}_{25}\text{Pt}_{75}$ and $\text{Ni}_{75}\text{Pt}_{25}$ compounds in $L12$ structures are calculated for comparison. We then investigate the efficacy of ordered-alloy force constants in reproducing the spectrum of the random 50-50 alloy. Concluding remarks appear in Sec. IV.

II. THEORETICAL BACKGROUND

A. Details of first-principles calculations

In what follows we report computations of the ground-state properties and phonon spectra of $\text{Ni}_{50}\text{Pt}_{50}$ ordered alloys in the $L10$ structure. We consider two cases. In the first, the c/a ratio of the tetragonal $L10$ structure is set equal to unity and only the volume is relaxed. We have referred to this structure above as “pseudocubic” and below it is simply referred to as “cubic.” In the second, the c/a ratio is relaxed as well. Structural information and force constant data for pure Ni and Pt and ordered Ni_3Pt and NiPt_3 are also presented. We use density-functional theory within the local-density approximation (LDA) to relax the different structures. We employ a plane-wave pseudopotential approach with the Perdew-Zunger parametrization²⁵ of the LDA as implemented in the PWSCF package.²⁸ Ultrasoft pseudopotentials²⁹ are used for Ni and Pt and explicitly treat ten valence electrons for each species with a kinetic energy cutoff of 30 Ry. Nonlinear core corrections are included in the Ni pseudopotential.³⁰ The Brillouin zone (BZ) integrations are carried out with Methfessel-Paxton smearing³¹ using an $8 \times 8 \times 8$ \mathbf{k} -point mesh, which corresponds to 70 \mathbf{k} points in the irreducible wedge. The value of the smearing parameter is 0.03 Ry. Hellmann-Feynman forces are calculated, and the atoms are relaxed steadily toward their equilibrium values until the forces are less than 1 mRy/a.u.. These parameters are found to yield phonon frequencies converged to within 5 cm^{-1} .

Once adequate convergence is achieved for the ground-state structural properties, the phonon spectra are obtained from linear response using density-functional perturbation

theory (DFPT).³² Within the DFPT, the force constants are conveniently computed in reciprocal space on a finite \mathbf{q} -point grid; to obtain the real-space force constants, Fourier transforms are then performed numerically. The number of unique real-space force constants and their reliability depend on the density of the \mathbf{q} -point grid: the closer the \mathbf{q} points are spaced, the more accurate the force constants of the higher neighbors will be. In this work, the dynamical matrix is computed on a $6 \times 6 \times 6$ \mathbf{q} -point mesh commensurate with the \mathbf{k} -point mesh for all structures.³³

B. Itinerant coherent potential approximation

The itinerant coherent potential approximation is a Green’s-function-based technique for treating random substitutional alloys. It is capable of treating off-diagonal and environmental disorder and therefore appropriate for the study of phonons in alloys with strong force constant disorder. The ICPA was developed and used to study $\text{Ni}_{55}\text{Pd}_{45}$ and $\text{Ni}_{50}\text{Pt}_{50}$ alloys.¹⁹ The recent results of Ref. 19 demonstrate its advantages over the simpler CPA for understanding both the dispersion and lifetimes of phonons in random binary alloys. However, in that work empirical force constants were adjusted to fit frequencies and linewidths extracted from neutron-scattering data. Using DFPT to calculate the phonon frequencies and force constants of various ordered structures allows us to make a series of comparisons with both the empirical force constant results and experiment. In doing so, we test the extent to which ordered-alloy force constants resemble random-alloy force constants and thereby illuminate the effect of relaxation on force constants, as reported in the next section.

III. RESULTS AND DISCUSSION

A. Structural information and ground-state properties

Solid elemental nickel and platinum stabilize in the fcc structure under standard conditions and are mutually soluble at all concentrations. When combined, they form ordered compounds at 1:3, 1:1, and 3:1 Ni:Pt atomic proportions. The 1:3 and 3:1 phases crystallize in the cubic $L12$ (Cu_3Au) structure; the 1:1 phase takes up the $L10$ crystal structure³⁴ as shown in Fig. 1. All of these structures contain four atoms per unit cell. Their electronic structures, ordering tendencies, and magnetic properties have been investigated in detail over the years.³⁵

In Table I, we report the equilibrium lattice parameters for the three compounds obtained from first-principles calculations performed as described above and compare them with the experimental data.³⁶ The LDA lattice parameters are 1–2 % less than the experimental values, which is within the normal range of error of the LDA and qualifies as very satisfactory agreement.

B. Phonon spectra

The phonon spectrum of the 50-50 ordered alloy in the $L10$ structure consists of 12 branches, three acoustic and nine optical. The results of our first-principles DFPT calculations

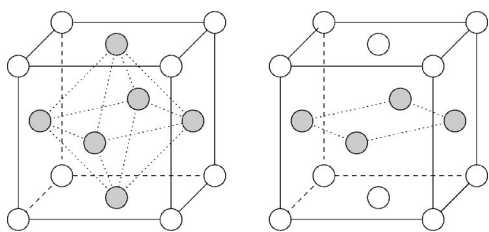


FIG. 1. Schematic $L12$ (left) and “cubic” (right) structures. For Ni_3Pt the white circles in the $L12$ structure indicate Pt atoms, the gray ones Ni, and vice versa for $NiPt_3$. The white circles in the “cubic” structure indicate Pt atoms, the gray ones Ni atoms. In the $L12$ structure, atoms of each species form three-dimensional next-neighbor networks; the “cubic,” on the other hand, is a layered structure of Ni-Pt layers in the (001) direction with $c=a$. In the $L10$ structure c/a is free to relax, allowing an adjustment of the Ni-Pt layer separation.

are shown along the high-symmetry lines of the simple cubic BZ in the top panel of Fig. 2 for the “cubic” structure, i.e., $L10$ with $c=a$. Results for the fully relaxed $L10$ structure are shown in the bottom panel of Fig. 2. The corresponding densities of states (total and component projected) are shown on the right hand side of each figure.

Although many features of the “cubic” and $L10$ dispersion curves are similar, several key differences emerge upon close examination. The frequencies of the optical branches in all three principal directions Γ - X , Γ - M , and Γ - R are higher in $L10$ than in the “cubic” arrangement. Indeed, since the unrelaxed “cubic” structure has a slightly larger volume than the $L10$ (by roughly 0.5%), it would be expected to possess frequencies that are, in an average sense, smaller than those seen in the $L10$. Comparing the eigenvectors and the projected densities of states of the two structures, we find that, for both structures, the longitudinal optical branches are heavily dominated by the vibrations of the lighter Ni atoms, and the acoustic modes are rich in the motions of heavier Pt atoms, again as expected. However, closer scrutiny of the $L10$ dispersion curves reveals a much more appreciable Pt contribution at intermediate frequencies (~ 4 -5 THz). The enhanced Ni-Pt mixing at these frequencies is consistent with the fact that in $L10$, the interplanar distance decreases from 4.9427 to 3.335 a.u.

In the “cubic” structure, component-projected densities of states indicate that low-frequency phonons are dominated by

TABLE I. Lattice parameters of NiPt ordered compounds calculated using DFPT and compared to experimental values taken from Ref. 36. “Cubic” refers to the lattice constant a of the NiPt structure obtained by fixing c/a at unity.

System	a (a.u.)	Expt.	c/a	Expt.
Ni	6.480	6.650		
Ni_3Pt	6.744	6.892		
$L10$ NiPt	7.136	7.244	0.934	0.939
“cubic” NiPt	6.99			
$NiPt_3$	7.200	7.320		
Pt	7.394	7.410		

Pt and the high-frequency phonons are dominated by Ni, with very little evidence of available states around the middle. This stricter separation of the Ni and Pt contributions is the signature of split-band behavior. Since no such split-band behavior is seen in random $Ni_{50}Pt_{50}$ alloy,¹⁹ the force constants computed from the “cubic” structure would not be expected to represent those of the random alloy. Relaxing to $L10$, on the other hand, results in contributions from both Ni and Pt in the low-frequency acoustic branches across the Brillouin zone, consistent with the appearance of more states in the middle of the spectrum; the branches are more evenly distributed in energy. Similarly, the optical branches, also very closely spaced in the “cubic” structure, are seen to broaden in $L10$. These results illustrate how structural relaxation modifies the vibrational spectra of the ordered alloy, bringing it closer to that of the disordered alloy within which atomic relaxation is less constrained.

Table II lists the computed real-space force constants for the elements, the ordered phases, and, for comparison, the empirical force constants of Ref. 19 for the disordered 50-50 alloy. We first consider the composition dependence of the force constants of the fully relaxed structures in the sequence Pt, $NiPt_3$, $L10$ NiPt, Ni_3Pt , and Ni. All Pt-Pt and Ni-Ni force constants increase monotonically in magnitude with Ni concentration; the Pt-Pt and Ni-Ni nearest-neighbor separations decrease concomitantly, compressing the atoms, roughly speaking, and causing the force constant increase. The Pt-Pt force constants, however, increase substantially less than the Ni-Ni force constants. The ratio of maximum to minimum force constants ranges from 1.24 (zz component) to 1.47 (xx) for Pt-Pt, whereas that for Ni-Ni ranges from 2.28 (xy) to 3.34 (zz). We note also that the composition dependence of the Ni-Pt force constants is weakly nonmonotonic for the zz and xy components with little difference in all three force constants between their values from $NiPt_3$ and $L10$ NiPt.

In Ref. 19, an excellent fit to the experimental coherent and incoherent inelastic scattering cross sections at the 50-50 composition was obtained through adjustment of the measured Ni-Ni, Ni-Pt, and Pt-Pt nearest-neighbor (NN) force constants. In particular, the Ni-Ni NN force constants had to be reduced well below their experimental values in pure Ni to obtain good agreement, while adjusting the Pt-Pt NN force constants was found to be substantially less effective in modifying the cross sections. The Pt-Pt force constants were thus modified only slightly from their experimental values in pure Pt, as seen in Table II. (Details of the fitting strategy are given in Ref. 19.) This receives some *post hoc* justification given the relative insensitivity of the Pt-Pt NN force constants to composition manifest in Table II and noted above. We comment further in the next section on the implications of the sequence of force constants for the three 50-50 compositions in the table.

C. Ordered-alloy force constants as a first approximation to the disordered alloy

A detailed understanding of phonon excitations in disordered alloys has been impeded by absence of detailed knowledge of the force constants. Even in the case of substitutional

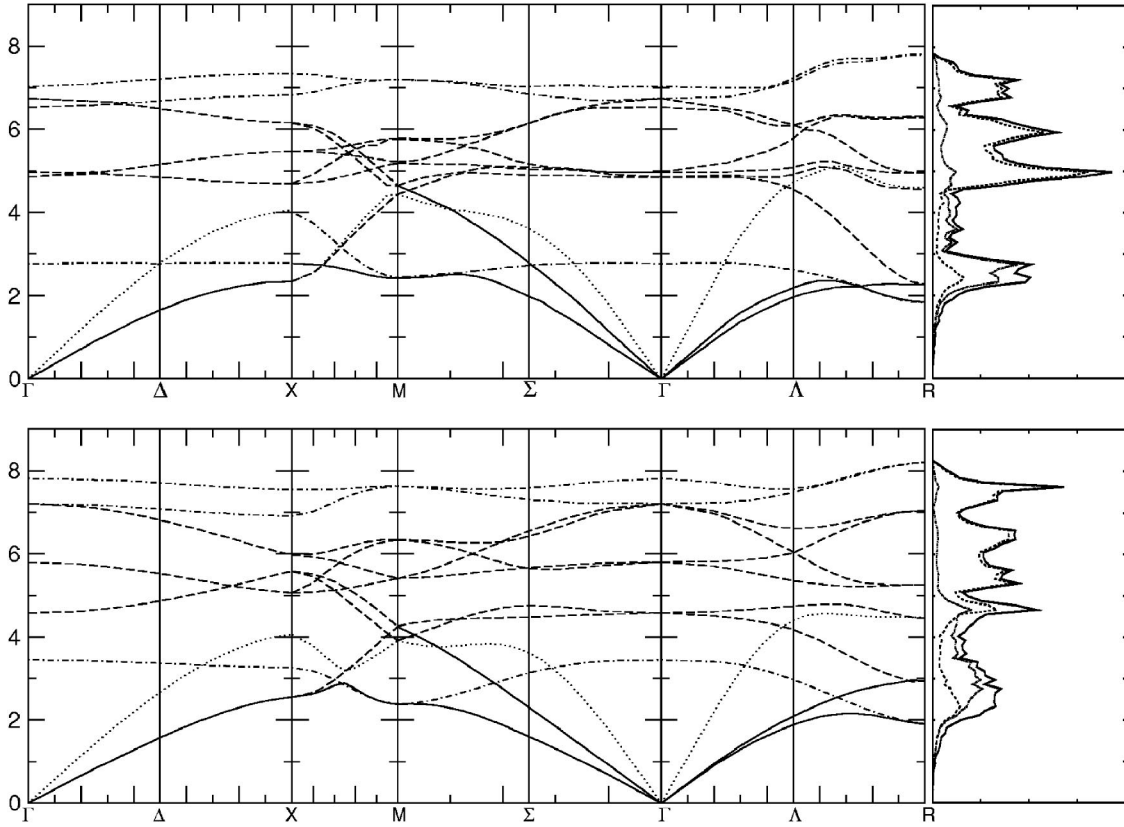


FIG. 2. Dispersion curves and phonon densities of states for “cubic” NiPt (top) and relaxed NiPt in the $L10$ structure (bottom), calculated from DFPT within the LDA. The leftmost panels are the dispersion curves along high-symmetry points in the Brillouin zone. The panels on the right are the total and component-projected densities of states. In the panels showing the dispersion curves, the solid lines are the transverse acoustic modes, the dotted lines are the longitudinal acoustic modes, the dot-dashed lines are the longitudinal optical modes, and the long-dashed lines are the transverse optical modes. In the panels showing the densities of states, the dashed lines are the Ni contributions, the dotted lines the Pt contributions, and the solid lines the total contributions to the densities of states.

disorder, the atoms have the freedom to relax, and, due to the random occupation of sites, the interactions among various species are expected to be quite different from those in the ordered alloy.

To explore the impact of lattice relaxation on the force constants, we calculate the incoherent inelastic scattering cross-section of the random NiPt alloy using the first-

principles force constants of the unrelaxed “cubic” structure and the fully relaxed $L10$ structure. The results are shown in Fig. 3. Note that the “cubic” curve is considerably higher than the data at low frequencies, and lower at high frequencies. These discrepancies are substantially reduced by relaxation: the force constants from $L10$ markedly improve the agreement between experiment and theory. Detailed differ-

TABLE II. Real-space nearest-neighbor force constants for the elements and the three compounds calculated with DFPT; the empirical (emp) force constants of Ref. 19 for the random NiPt alloy are included for comparison. The units are dyn cm^{-1} .

	Pt	NiPt ₃	“Cubic” NiPt	$L10$ NiPt	NiPt (emp)	Ni ₃ Pt	Ni	
Ni-Ni			-4863	-5252	-15587	-11758	-13800	1xx
Ni-Pt		-13200	-17418	-13279	-13855	-29762		1xx
Pt-Pt	-27744	-37571	-51175	-40158	-28993			1xx
Ni-Ni			318	498	436	253	149	1zz
Ni-Pt		2813	2171	2643	348	3044		1zz
Pt-Pt	5512	5559	9486	6623	7040			1zz
Ni-Ni			-5373	-6801	-19100	-13028	-15530	1xy
Ni-Pt		-15949	-21885	-15859	-15280	-35310		1xy
Pt-Pt	-30969	-40474	-59322	-45529	-30317			1xy

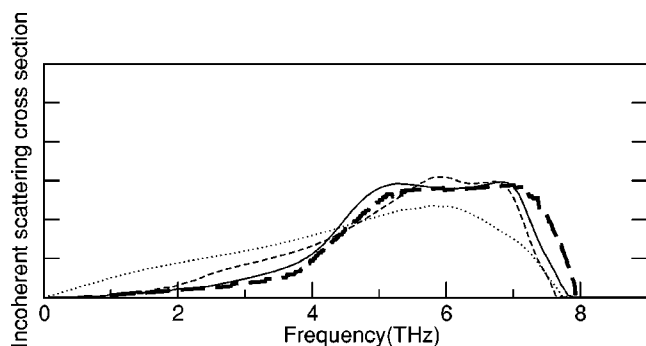


FIG. 3. Inelastic incoherent scattering cross sections for $\text{Ni}_{50}\text{Pt}_{50}$ random alloy. The solid line is the experimental result, the bold dashed line is the ICPA result with empirical force constants, the dashed line is the ICPA result with first-principles force constants for $L10$ NiPt, and the dotted line is the ICPA results with first-principles force constants for “cubic” NiPt.

ences do remain between the $L10$ and the experimental curves, however. In particular, the cross section is still higher than the data at low frequencies (below about 4 THz), and the high-frequency cutoff predicted from the $L10$ force constants is lower than measured, a disagreement unchanged by relaxation. We attribute these discrepancies to the constraints on relaxation enforced by the order on the nearest-neighbor separations. In the random alloy such constraints are obviously absent, and force constants computed from larger supercells averaged over several configurations may improve the agreement. For example, allowing the Ni-Ni NN separation to drop below that predicted from our ordered $L10$ structure would increase the Ni-Ni force constants, shifting spectral weight from lower to higher frequency in Fig. 3 and improving the agreement with the empirical force constants in Table II. Similarly, the Pt-Pt nn separation can increase, which would tend to reduce the Pt-Pt force constants toward their empirical values in Table III. The case of the Ni-Pt force constants is more subtle. The Pt-Pt force constants are larger in magnitude than the Ni-Ni force constants, which suggests that the energetic cost of compressing Pt is larger than that of expanding Ni. This suggests in turn that the Ni-Pt separation increases in the random alloy, which would also reduce the Pt-Ni force constants, as we find.

Several other interesting trends can be seen in the force constants. The lattice constant of the “cubic” NiPt alloy is 6.99 a.u. Due to the contraction of the “cubic” lattice relative to the tetragonal $L10$ structure, the larger Pt atoms have less space to vibrate, resulting in a stiffening of the Pt-Pt interaction, as can be seen in Table II. In contrast, since Ni is a relatively much smaller ion than Pt, the Ni-Ni interaction does not significantly change. For this reason we predict too much weight in the low-frequency region of the scattering cross section in Fig. 3. The low-frequency region is dominated by Pt atoms and, due to the considerable hardening of Pt-Pt compared to Ni-Ni, the Pt-Pt interaction dominates throughout the entire frequency spectrum for “cubic” NiPt. After relaxation to the $L10$ structure, the situation improves. The atomic separation in the Ni and Pt planes grows (since the in-plane lattice parameter increases), softening the Pt-Pt interactions and producing better agreement with the experi-

ment. These results underline the importance of capturing relaxation effects in random environments.

While we have captured *some* of the relaxation occurring in the random alloy, a deficiency of our theory is certainly that we fail to capture *all* of it. For example, we neglect randomness in the relaxation, and this may be responsible for our underestimate of the position of the high-frequency band edge in Fig. 3. As mentioned, the Ni-Ni interaction is still too weak to push the upper band edge toward higher frequency. It also has to be noted that the shapes and the features of the two scattering cross section curves obtained by the ICPA using the “cubic” and $L10$ force constants have very little similarity, implying that structural relaxation is even more pronounced in random alloys than in ordered systems as stated above. The incoherent scattering cross sections are nothing but the component-projected densities of states weighted by their incoherent scattering lengths and therefore carry the signature of the component-projected densities of states. Figure 2 suggests that, although quite dissimilar in their various features, there is more overall similarity in the densities of states curves for the ordered structures than in their random counterpart.

Since the use of $L10$ ordered-alloy force constants improves agreement with experiment, it is tempting to follow the same procedure for $\text{Ni}_x\text{Pt}_{1-x}$ at $x=0.25$ and $x=0.70$, other concentrations at which experiments have been done. However, in the simplest ordered counterpart of $\text{Ni}_{25}\text{Pt}_{75}$, a Ni atom does not have any Ni nearest neighbors and the Ni-Ni force constant has to be estimated empirically. Moreover, $\text{Ni}_{70}\text{Pt}_{30}$ does not even have a simple ordered counterpart. Thus the agreement for the 50-50 case may be of limited general use. The force constant data in Table II, however, suggest that the Ni-Ni and Pt-Pt force constants vary approximately linearly with composition, following a Vegard’s law of sorts for force constants. Assuming this holds throughout the concentration range, one could then easily interpolate to an arbitrary concentration and use the results as a reasonable first guess for force constants at that particular concentration. On the other hand, the Ni-Pt force constants are approximately the same for NiPt₃ and NiPt($L10$), justifying a linear interpolation for starting values for the $\text{Ni}_{30}\text{Pt}_{70}$ alloy.

As alluded to above, another route would be to consider more complicated ordered structures. Zunger and collaborators have demonstrated that a clever choice of supercell plus additional relaxation can reliably reproduce the optical and thermodynamic properties of certain binary alloys.^{24,37} Their supercell was constructed by arranging a minimal set of atoms so that the first few peaks of the radial correlation function match those of the disordered alloy for a given concentration. Despite a plethora of works successfully using these and simpler atomic arrangements to model the properties of alloys, to our knowledge there has yet to be a study assessing the ability of *any* of these structures to reproduce the details of the phonon spectra of random alloys. In a subsequent communication, we shall examine the utility of using such an artificial supercell to obtain force constants in a random environment.

IV. CONCLUSIONS

In an attempt to reach the greater goal of obtaining reliable first-principles force constants for Ni₅₀Pt₅₀ alloys, we have studied the vibrational properties of ordered stoichiometric compounds of Ni and Pt using first-principles DFPT. The analysis of the phonon spectra based on the interactions between different constituents of the alloy and their variations under different environments provides useful insight about those interactions in random environments. The calculated force constants of compounds of different stoichiometry

elucidate two other important features of the force constants: first, they provide a *posteriori* validation of our choice of phenomenological force constants¹⁹ for Ni₅₀Pt₅₀; and second, they clarify the composition-dependent variation of the force constants of ordered, stoichiometric compounds. This paves the way to reasonable estimates of off-stoichiometric force constants at arbitrary concentration. Most importantly, this study strongly suggests that a successful theoretical description of the vibrational properties of random alloys must include the effects of atomic relaxation.

*Present address: Department of Materials Science & Engineering, University of Illinois at Urbana-Champaign, Urbana, IL 61801, USA.

†Present address: The Molecular Foundry, Materials Sciences Division, Lawrence Berkeley National Laboratory, Berkeley, CA 94720, USA.

‡Present address: Institut of Solid State Research (IFF), Research Centre Jülich, 52425 Jülich, Germany.

- ¹B. Mozer, K. Otnes, and V. W. Myers, Phys. Rev. Lett. **8**, 278 (1962); B. Mozer, K. Otnes, and C. Thaper, Phys. Rev. **152**, 535 (1966); E. C. Svensson, B. N. Brockhouse, and J. M. Rowe, Solid State Commun. **3**, 245 (1965); E. C. Svensson and B. N. Brockhouse, Phys. Rev. Lett. **18**, 858 (1967); H. G. Smith and M. K. Wilkinson, *ibid.* **20**, 1245 (1968); R. M. Nicklow, P. R. Vijayraghavan, H. G. Smith, and M. K. Wilkinson, in *Neutron Inelastic Scattering* (IAEA, Vienna, 1968), Vol. I, p. 47.
- ²R. M. Cunnigham, L. D. Muhlestein, W. M. Shaw, and C. W. Tompson, Phys. Rev. B **2**, 4864 (1970); N. Wakabayashi, R. M. Nicklow, and H. G. Smith, *ibid.* **4**, 2558 (1971); E. C. Svensson and W. A. Kamitakahara, Can. J. Phys. **49**, 2291 (1971); N. Wakabayashi, Phys. Rev. B **8**, 6015 (1973); B. N. Brockhouse and R. M. Nicklow, Bull. Am. Phys. Soc. **18** (1), 112 (1973); A. Zinken, U. Buchenau, H. J. Fenzel, and H. R. Schober, Solid State Commun. **13**, 495 (1977).
- ³W. A. Kamitakahara and B. N. Brockhouse, Phys. Rev. B **10**, 1200 (1974).
- ⁴Y. Tsunoda, N. Kunitomi, N. Wakabayashi, R. M. Nicklow, and H. G. Smith, Phys. Rev. B **19**, 2876 (1979).
- ⁵R. M. Nicklow, in *Methods of Experimental Physics* (Academic Press, New York, 1983), Vol. 23, p. 172.
- ⁶D. H. Dutton, B. N. Brockhouse, and A. P. Miller, Can. J. Phys. **50**, 2915 (1972).
- ⁷G. A. DeWit and B. N. Brockhouse, J. Appl. Phys. **39**, 451 (1968).
- ⁸S. de Gironcoli, Phys. Rev. B **51**, 6773 (1995).
- ⁹D. W. Taylor, Phys. Rev. **156**, 1017 (1967).
- ¹⁰N. Kunimoto, Y. Tsunoda, and Y. Hirai, Solid State Commun. **13**, 495 (1973); T. Kaplan and M. Mostoller, Phys. Rev. B **9**, 353 (1974); W. A. Kamitakahara, Bull. Am. Phys. Soc. **19** (1), 321 (1974); R. J. Elliot, J. A. Krumhansl, and P. L. Leath, Rev. Mod. Phys. **46**, 465 (1974).
- ¹¹W. A. Kamitakahara and D. W. Taylor, Phys. Rev. B **10**, 1190 (1974); M. Mostoller, T. Kaplan, N. Wakabayashi, and R. M. Nicklow, *ibid.* **10**, 3144 (1974); H. G. Smith and N. Wakabayashi, Bull. Am. Phys. Soc. **21** (1), 410 (1976).
- ¹²H. Shiba, Prog. Theor. Phys. **40**, 942 (1968).

¹³T. Kaplan and M. Mostoller, Phys. Rev. B **9**, 1783 (1974).

¹⁴S. Takeno, Prog. Theor. Phys. **40**, 942 (1968).

¹⁵B. G. Nickel and W. H. Butler, Phys. Rev. Lett. **30**, 373 (1973).

¹⁶F. Ducastelle, J. Phys. C **7**, 1795 (1974); J. Mertsching, Phys. Status Solidi B **63**, 241 (1974).

¹⁷A. Gonis and J. W. Garland, Phys. Rev. B **18**, 3999 (1978).

¹⁸M. Yussouff and A. Mookerjee, J. Phys. C **17**, 1009 (1984).

¹⁹S. Ghosh, P. L. Leath, and M. H. Cohen, Phys. Rev. B **66**, 214206 (2002).

²⁰A. Zunger and J. E. Jaffe, Phys. Rev. Lett. **51**, 662 (1983).

²¹J. E. Bernard and A. Zunger, Phys. Rev. B **34**, 5992 (1986).

²²A. A. Mbaye, L. G. Ferreira, and A. Zunger, Phys. Rev. Lett. **58**, 49 (1987).

²³A. Sher, M. van Schilfgarde, A. B. Chen, and W. Chen, Phys. Rev. B **36**, 4279 (1987).

²⁴S. H. Wei, L. G. Ferreira, J. E. Bernard, and A. Zunger, Phys. Rev. B **42**, 9622 (1990).

²⁵P. Weightman, H. Wright, S. D. Waddington, D. van der Marel, G. A. Sawatzky, G. P. Diakun, and D. Norman, Phys. Rev. B **36**, 9098 (1987).

²⁶G. Renaud, N. Motta, F. Lancon, and M. Belakhovsky, Phys. Rev. B **38**, 5944 (1988).

²⁷J. P. Perdew and A. Zunger, Phys. Rev. B **23**, 5048 (1981).

²⁸S. Baroni, A. Dal Corso, S. de Gironcoli, and P. Giannozzi, <http://www.pwscf.org>

²⁹D. Vanderbilt, Phys. Rev. B **41**, 7892 (1990).

³⁰S. G. Louie, S. Froyen, and M. L. Cohen, Phys. Rev. B **26**, 1738 (1982).

³¹M. Methfessel and T. A. Paxton, Phys. Rev. B **40**, 3616 (1989).

³²S. Baroni, P. Giannozzi, and A. Testa, Phys. Rev. Lett. **58**, 1861 (1987).

³³P. Giannozzi, S. de Gironcoli, P. Pavone, and S. Baroni, Phys. Rev. B **43**, 7231 (1991).

³⁴M. C. Cadeville and J. L. Moran-Lopez, Phys. Rep. **153**, 331 (1987).

³⁵A. Pistany, C. Amador, Y. Ruiz, and M. de la Vega, Z. Phys. B: Condens. Matter **80**, 237 (1990); J. Staunton, P. Weinberger, and B. L. Gyorffy, J. Phys. F: Met. Phys. **13**, 779 (1983); B. L. Gyorffy and G. M. Stocks, Phys. Rev. Lett. **50**, 374 (1983); F. J. Pinski, B. Ginatempo, D. D. Johnson, J. B. Staunton, G. M. Stocks, and B. L. Gyorffy, *ibid.* **66**, 766 (1991).

³⁶C. E. Dahmani, Ph.d. thesis, Universite Louis Pasteur, Strasbourg, 1985.

³⁷A. Zunger, S. H. Wei, L. G. Ferreira, and J. E. Bernard, Phys. Rev. Lett. **65**, 353 (1990).